

Pulmonary Vascular Resistance and Impedance in Isolated Mouse Lungs: Effects of Pulmonary Emboli

HOLLY A. TUCHSCHERER, EIDAN B. WEBSTER, and NAOMI C. CHESLER

Department of Biomedical Engineering, University of Wisconsin, Madison, WI 53706-1609

(Received 25 August 2004; accepted 24 October 2005; published online: 28 March 2006)

Abstract—To study pulsatile pressure-flow rate relationships in the intact pulmonary vascular network of mice, we developed a protocol for measuring pulmonary vascular resistance and impedance in isolated, ventilated, and perfused mouse lungs. We used pulmonary emboli to validate the effect of vascular obstruction on resistance and impedance. Main pulmonary artery and left atrial pressures and pulmonary vascular flow rate were measured under steady and pulsatile conditions in the lungs of C57BL/6J mice ($n = 6$) before and after two infusions with 25 μm -diameter microspheres (one million per infusion). After the first and second embolizations, pulmonary artery pressures increased approximately two-fold and three and a half-fold, respectively, compared to baseline, at a steady flow rate of 1 ml/min ($P < 0.05$). Pulmonary vascular resistance and 0 Hz impedance also increased after the first and second embolizations for all flow rates tested ($P < 0.05$). Frequency-dependent features of the pulmonary vascular impedance spectrum were suggestive of shifts in the major pulmonary vascular reflection sites with embolization. Our results demonstrate that pulmonary artery pressure, resistance, and impedance magnitude measured in this isolated lung setup changed in ways consistent with *in vivo* studies in larger animals and humans and demonstrate the usefulness of the isolated, ventilated, and perfused mouse lung for investigating steady and pulsatile pressure-flow rate relationships.

Keywords—Microspheres, Pulmonary embolism, Impedance spectrum, Right ventricular hydraulic afterload, Murine.

INTRODUCTION

In pulmonary hypertension, the pressure and flow characteristics of the pulmonary vascular system deviate from the normal state. Pulmonary vascular resistance and pulmonary vascular impedance are two of the parameters typically calculated to estimate the severity of pulmonary hypertension, and to predict the increased work and stress on the heart.^{15,20,21} In particular, resistance and impedance have been measured in animal models such as rats, dogs, goats, and pigs.^{8,11,18,22,32} To our knowledge, the effects

of pulmonary hypertension on pulsatile pressure-flow rate relationships in mice have not been investigated.

Isolated, ventilated, and perfused mouse lungs have been used to investigate pulmonary vascular reactivity and steady pressure-flow rate relationships in response to acute hypoxia^{9,12,34} and in the presence of genetic defects.^{1,10,17,27} Mice are an especially advantageous animal model for pulmonary research because knockout and transgenic mice, which are becoming more widely available, are valuable in studying the molecular mechanisms of pulmonary diseases. However, the small size of the mouse can make the task of obtaining quality *in vivo* data challenging. To date, only steady flow perfusion has been used in the isolated, ventilated, and perfused mouse lung, which limits the information about pressure-flow rate relationships that can be derived from these studies. To investigate frequency-dependent responses to pulmonary disease such as pulmonary hypertension, pulsatile flow at physiological frequencies must be used.

In this study, we created pulsatile pulmonary vascular flow, which is the analog of right ventricular output in a whole animal, with mechanical pumps that could produce a wide range of both steady and sinusoidal flow rates at physiological frequencies in a technique pioneered by Caro and McDonald.⁴ Consequently, we could measure the pulmonary vascular pressure-flow rate relationships for a range of flow magnitudes and pulsation frequencies in the isolated, ventilated, and perfused mouse lung. We measured these pressure-flow rate relationships before and after two rounds of pulmonary embolization with microspheres in order to validate the ability of the setup to quantify increases in resistance and impedance due to obstruction. In particular, based on the literature on *in vivo* studies in larger animals, we sought to demonstrate that emboli would increase pulmonary vascular resistance (PVR), increase impedance magnitude at 0 Hz (Z_0) and cause changes in high frequency impedance. We also investigated changes in the characteristic impedance Z_C , index of wave reflection R_w and frequency of the first minimum in the impedance magnitude (f_{\min}).

Address correspondence to Naomi C. Chesler, Department of Biomedical Engineering, University of Wisconsin-Madison, 2146 Engineering Centers Building, 1550 Engineering Drive, Madison WI 53706-1609. Electronic mail: chesler@engr.wisc.edu

METHODS AND MATERIALS

Animal Handling

Three female and three male 10–12 week old C57BL/6J mice, 24 ± 5 g weight were used (Jackson Laboratory, Bar Harbor, ME). Mice were anesthetized with an intraperitoneal injection of 150 mg/kg pentobarbital solution. All protocols and procedures were approved by the University of Wisconsin Institutional Animal Care and Use Committee.

Isolated Lung Preparation

After confirmation of deep anesthesia, the animal was placed in a chamber for isolated lung ventilation and perfusion (IL-1 system, Hugo Sachs Elektronik, March-Hugstetten, Germany). The chamber was heated to 37°C to maintain body temperature. A tracheotomy was performed, and a stainless steel ventilation cannula was inserted into the tracheal stoma. The distal trachea was secured to the cannula with suture. Thereafter, the animal was ventilated with room air at 90 breaths/min with peak inspiratory and expiratory pressures of 10 and 2 cm H_2O , respectively, and an inspiratory/expiratory ratio of 1:1, as previously reported.³¹ Airway pressure and airway flow rate were measured with pressure and flow transducers (MPX and Validyne 45–14, respectively, Hugo Sachs Elektronik). Deep breaths to 20 cm H_2O every 10 min were performed to prevent atelectasis.³¹

Then, a thoracotomy was performed and 500 U/100 g body weight heparin was injected into the right ventricle to prevent blood clotting. The animal was euthanized by exsanguination, and the lower abdomen removed. Once identified and isolated, the pulmonary artery was cannulated through an incision in the right ventricle and secured in place by a suture around the pulmonary artery. The left atrium was subsequently cannulated through an incision in the left ventricle. The left atrial cannula was positioned and held in place by the mitral valve ring without suture.

Thus instrumented, the lung vasculature was perfused with 3.5% Ficoll (Sigma-Aldrich, St. Louis, MO) in RPMI 1640 cell culture medium (Cellgro, Mediatech, Inc., Herndon, VA) preheated to 37°C . Steady flow was driven by a syringe pump (Cole Palmer Instrument Company, Vernon Hills, IL) and passed through a heat exchanger (at 37°C) and bubble trap before reaching the pulmonary artery. Pulsatile flow was driven by a high frequency oscillatory piston pump (EnduraTEC Systems Corporation, Minnetonka, MN) operated in parallel with the syringe pump. Flow exited the left atrium into approximately 20 cm of small diameter tubing (ID = 1.03 mm), which then exited to the atmosphere at the same elevation as the left atrial cannula. Thus, left atrial pressure was equal to the sum of atmospheric pressure and the viscous pressure drop in the tubing, which was linearly proportional to the flow rate. The lungs and heart

were routinely wetted with 1% phosphate buffered saline solution (PBS) spray. The lungs were kept on positive-pressure ventilation throughout the experiment. Pulmonary artery pressure (P_{PA}) and left atrial pressure (P_{LA}) were measured by pressure transducers (P75, Hugo Sachs Elektronik) connected to the pulmonary artery and left atrium cannulas by approximately 20 cm of small diameter (ID = 0.77 mm), nearly rigid tubing. Pulmonary vascular flow rate (Q) was measured by an in-line flowmeter (Transonic Systems, Inc., Ithaca, NY) placed approximately 6 cm upstream from the pulmonary artery cannula. All pressures and flows were monitored by continuous display (LabView 6.1, National Instruments, Austin, TX) on a laptop computer (Dell Latitude, Round Rock, TX). See Fig. 1 for schematic of the isolated, ventilated, and perfused lung setup.

Initial Measurements

To obtain initial steady flow rate measurements of P_{PA} , P_{LA} , and Q , the lungs were perfused at 1 ml/min until pressure stabilized, approximately 4–5 min. This perfusion rate was determined by previously reported flow rates for isolated perfused mouse lungs.³¹ Data were recorded for 5 s at 15 Hz, while keeping lungs inflated at the end-inspiratory pressure of 10 cm H_2O . Lungs were kept inflated to the end-inspiratory pressure during data collection to prevent edema and to normalize the effects of airway pressure and volume on P_{PA} , P_{LA} , and Q .²⁰

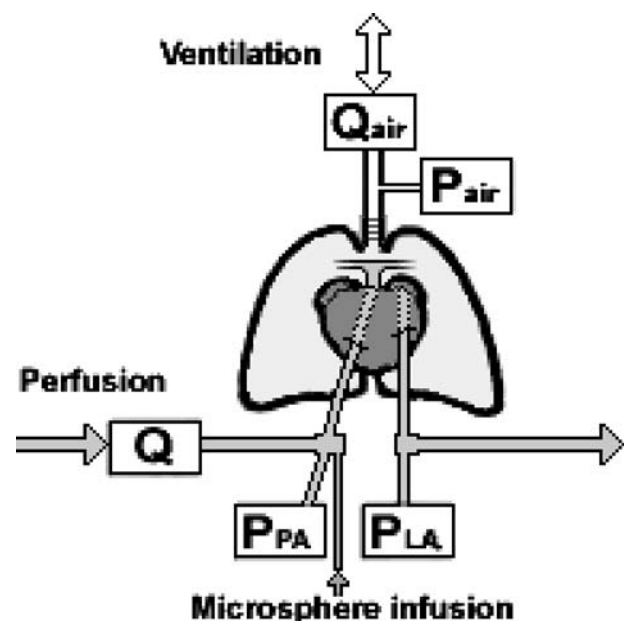


FIGURE 1. Isolated, ventilated, and perfused mouse lung setup showing cannulas and relative transducer locations for pulmonary artery pressure P_{PA} , left atrial pressure P_{LA} , perfusate flow rate Q , airway pressure P_{air} , and airway flow rate Q_{air} .

Pulsatile Flow Rate Measurements

The steady flow rate was gradually increased to 3 ml/min, and sinusoidal flow rates of the form $Q = 3 + 2 \sin(2\pi f t)$ ml/min were generated for frequencies $f = 1, 2, 5, 10, 15,$ and 20 Hz for a total of 22 s. This frequency range was chosen to include the physiological heart rate for mice (~ 10 Hz). P_{PA} , P_{LA} , and Q were recorded at 200 Hz. Similar to the initial steady flow rate measurements, lungs were kept inflated at end-inspiratory pressure (10 cm H_2O) during data collection. After the sinusoidal flow rate measurements were performed, the steady flow rate was gradually reduced to 0.5 ml/min and normal ventilation of 90 breaths/min resumed. The pulsatile flow rate measurements were repeated multiple times. Between repeated measurements, there was 1 min of steady flow at 0.5 ml/min with a ventilation rate of 90 breaths/min.

Steady Flow Rate Measurements

After the last pulsatile flow rate measurement, at least 1 min of steady flow at 0.5 ml/min was imposed, and then the flow rate was increased to 1 ml/min. The steady flow rate was then increased from 1 ml/min to 5 ml/min in 1 ml/min steps at 10 s intervals while P_{PA} , P_{LA} , and Q were recorded at 15 Hz. Lungs were inflated to end-inspiratory pressure during data collection as before. The steady flow rate was then reduced to 1 ml/min, and normal ventilation of 90 breaths/min resumed.

Addition of Microspheres

After the initial, pulsatile, and steady flow rate measurements, which constitute the baseline conditions for a given mouse lung, microspheres were infused into the pulmonary vasculature to simulate pulmonary embolism. Perfusion was set at 0.5 ml/min and ventilation was 90 breaths/min during the infusion. Approximately 1×10^6 25 μm polystyrene microspheres (crosslinked with divinylbenzene) with a coefficient of variance of 20% (Polysciences, Inc, Warrington, PA) were combined with 5 ml heated perfusion media (3.5% Ficoll in RPMI). The microsphere mixture was added at approximately 1 ml/min by syringe through a portal in the pulmonary artery cannula (see Fig. 1). Microspheres were sonicated before infusion to prevent clumping; however, some may have aggregated into clusters of 2 or 3 during the infusion. The initial, pulsatile, and steady flow rate measurements described above then were repeated to obtain the first embolization values. After these data were collected, another 1×10^6 microspheres were infused by the same method, and the second embolization values were acquired.

Lung Fixation and Histology

After all hemodynamic data were collected, the ventilation and perfusion were stopped and the lungs were re-

moved from the isolated lung system. The lungs were fixed with paraformaldehyde (3% in PBS) infused through the trachea; lungs were not inflated during infusion. Freezing compound OCT was then perfused through the trachea, and the entire lung was frozen in 2-methyl butane cooled by liquid nitrogen. Four sections with a thickness of 7 μm were cut from each lung at $-20^\circ C$ on a cryostat. The sections were stained with hematoxylin to indicate vascular and airway cell nuclei. Sections were imaged on an inverted microscope (TE-2000, Nikon, Melville, NY) and captured using a spot camera and software for image digitization (MetaVue, Optical Analysis Systems, Nashua NH).

Calculations

The pressure drop across the pulmonary vascular network (ΔP) was calculated as the pulmonary artery pressure minus the left atrial pressure ($P_{PA} - P_{LA}$). Under steady flow conditions, flow rate and pressures were averaged over 50 data points to obtain P_{PA} , ΔP , and Q for a given flow rate magnitude. Pulmonary vascular resistance (PVR) was calculated as $\Delta P/Q$.

Under pulsatile flow conditions, data obtained during one full sinusoidal cycle were analyzed at each frequency. Calculated parameters included impedance, characteristic impedance, input impedance, and index of wave reflection. The impedance was calculated in the frequency domain using fast Fourier transforms.²⁰ Specifically, the magnitude of the impedance (Z) was calculated as the ratio of the ΔP modulus to the Q modulus²⁴ using MATLAB (MathWorks, Inc., Natick, MA). The zeroth and first harmonic values were found for each imposed sinusoidal flow rate frequency. The phase angle between ΔP and Q waves for one cycle at each frequency, indexed to the time at which $Q = 3$ ml/min, was also analyzed using MATLAB. Characteristic impedance (Z_C) was calculated as the average of the impedance magnitudes between the first minimum (5 Hz at baseline) and 20 Hz.¹⁹ The same 5–20 Hz range was used to calculate Z_C after the first and second embolizations. The average impedance at the zeroth harmonic ($f = 0$ Hz) for all frequencies was taken as the input resistance (Z_0). The index of wave reflection (R_w) was calculated using $R_w = (Z_0 - Z_C)/(Z_0 + Z_C)$.²⁰

Statistics

Data were analyzed using a paired-Wilcoxon signed rank test. P -values less than 0.05 were considered significant. No differences were observed between male and female mice so all data were grouped. Statistical analyses were performed using SAS statistical software (SAS Institute Inc., Cary, NC). All data are presented in terms of mean value \pm standard deviation.

RESULTS

Initial Measurements

At baseline conditions, the initial measurement of P_{PA} was 11 ± 1 mmHg at 1 ml/min flow rate (Fig. 2). In response to the first and second infusions of microsphere emboli, P_{PA} increased significantly ($P < 0.05$ compared to baseline for both). Under all conditions, the pressures measured initially were higher than those measured with steady perfusion but after pulsatile flow (see Fig. 3 at 1 ml/min).

Steady Flow Rate Measurements

Under all conditions, P_{PA} increased as flow rate increased from 1 to 5 ml/min (Fig. 3). The dependence of P_{PA} on flow rate was well described by a power law function (as suggested by²⁸) at baseline and after the first and second embolizations ($R^2 > 0.98$ for all conditions). In all cases, P_{LA} increased approximately linearly due to the Poiseuille-type losses in the outflow tubing. After both the first and second embolizations, P_{PA} values were higher than baseline for all flow rates tested ($P < 0.05$). Compared to the first embolization, P_{PA} and the change in P_{PA} with a change in Q were greater after the second embolization, but the differences were not significant.

PVR was 7.7 ± 0.6 mmHg ml⁻¹ min at 1 ml/min under baseline conditions and decreased as flow rate increased from 1 to 5 ml/min ($P < 0.05$ between all flow rates) (Fig. 4). After both the first and second embolizations, PVR also decreased with increasing flow rate ($P < 0.05$). After both the first and second embolizations, PVR values were higher than baseline for all flow rates tested ($P < 0.05$). There were increases in the average PVR at all flow rates between the first and second embolizations, but they were not significant.

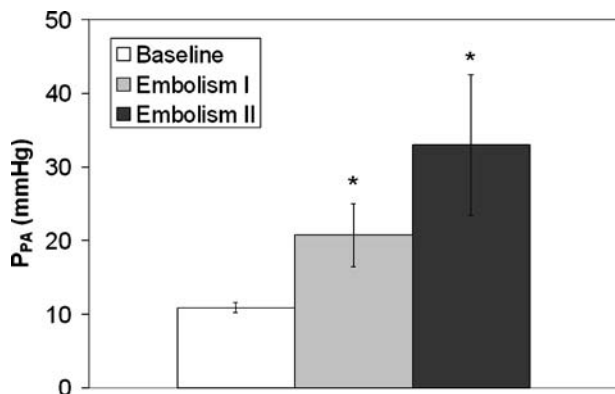


FIGURE 2. Initial measurements of pulmonary artery pressure P_{PA} for steady perfusion at baseline and after the first and second embolizations at 1 ml/min. Bars represent mean \pm standard deviation ($n = 6$). * $P < 0.05$ vs. baseline.

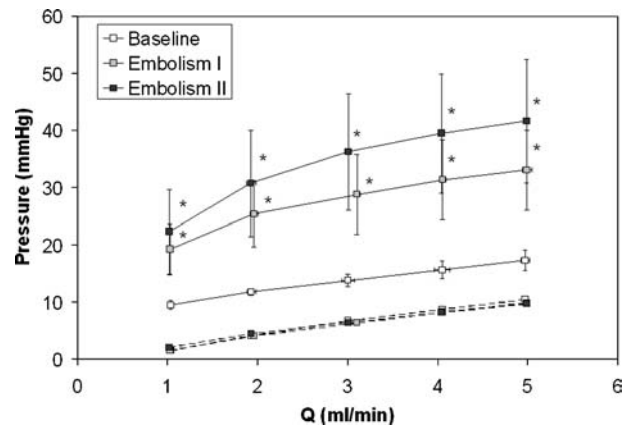


FIGURE 3. Pulmonary artery pressure P_{PA} (solid lines) and left atrial pressure P_{LA} (dashed lines) versus flow rate Q for steady perfusion at baseline and after the first and second embolizations. Bars represent mean \pm standard deviation ($n = 6$). * $P < 0.05$ vs. baseline.

Pulsatile Flow Rate Measurements

Under baseline conditions, average 0 Hz impedance magnitude, or input resistance (Z_0) was 2.1 ± 0.4 mmHg ml⁻¹ min and increased significantly after both the first and second embolizations ($P < 0.05$, Fig. 5). Impedance magnitudes at frequencies above 0 Hz were much lower than those at 0 Hz and were significantly different after embolization at high frequencies. The impedance phase was significantly more negative after embolization up to 10 Hz ($P < 0.05$); there were no differences at 15–20 Hz (Fig. 5).

The impedance magnitude data above 0 Hz were re-plotted to highlight the differences at nonzero frequencies (Fig. 6). At low frequencies (1–5 Hz), impedance magnitude (Z) showed little variation as a function of frequency at

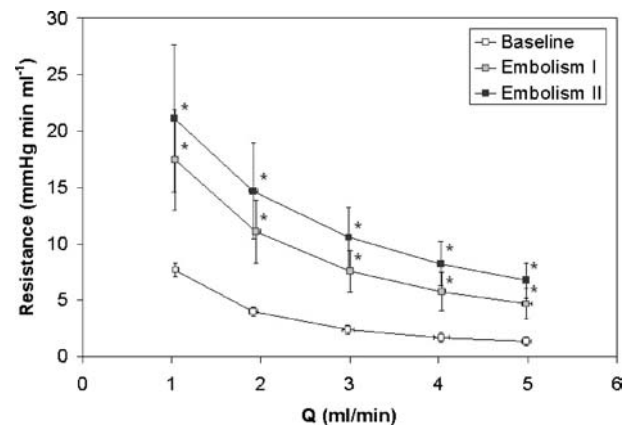


FIGURE 4. Pulmonary vascular resistance versus flow rate Q for steady perfusion at baseline and after the first and second embolizations. Bars represent mean \pm standard deviation ($n = 6$). * $P < 0.05$ vs. baseline.

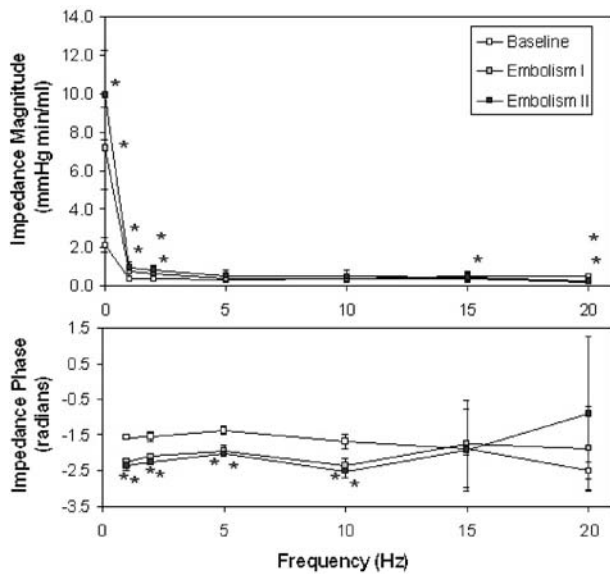


FIGURE 5. Pulmonary vascular impedance magnitude and phase versus frequency at baseline and after the first and second embolizations. The pulmonary vascular perfusate flow was $Q = 3 + 2 \sin(2\pi f t)$ ml/min for $f = 1, 2, 5, 10, 15,$ and 20 Hz, and data were recorded at the end-inspiratory pressure of 10 cm H_2O . Bars represent mean \pm standard deviation ($n = 6$). * $P < 0.05$ vs. baseline.

baseline. As frequency increased, Z also increased; values at 10 – 20 Hz were slightly but significantly larger than the 5 Hz value ($P < 0.05$). The first minimum of impedance magnitude (f_{\min}) was at 5 Hz. After both the first and second embolizations, Z was high at low frequencies and low at high frequencies. In particular, Z values at low frequencies (1 – 2 Hz) were significantly higher than values at high frequencies (10 – 20 Hz) ($P < 0.05$); f_{\min} was equal to or

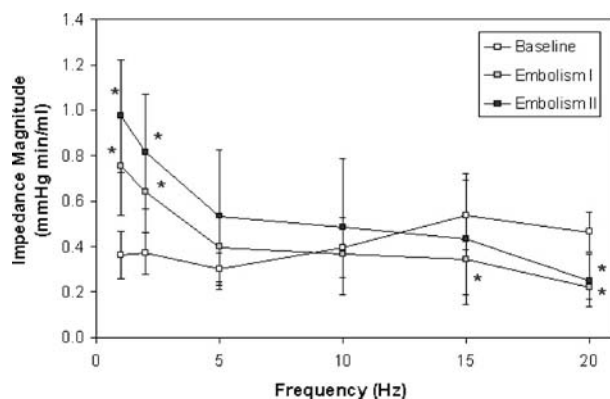


FIGURE 6. Pulmonary vascular impedance magnitude for frequencies above 0 Hz at baseline and after the first and second embolizations. The pulmonary vascular perfusate flow was $Q = 3 + 2 \sin(2\pi f t)$ ml/min for $f = 1, 2, 5, 10, 15,$ and 20 Hz, and data were recorded at the end-inspiratory pressure of 10 cm H_2O . Bars represent mean \pm standard deviation ($n = 6$). * $P < 0.05$ vs. baseline.

greater than 20 Hz. Also, at low frequencies (1 – 2 Hz), Z after both embolizations were higher than at baseline ($P < 0.05$) whereas at high frequencies (15 – 20 Hz), the reverse was true. Also, the impedance magnitudes after the second embolization were higher than those after the first embolizations at all frequencies.

Characteristic impedance (Z_C) was 0.43 ± 0.10 mmHg ml^{-1} min at baseline and decreased slightly to 0.31 ± 0.11 and 0.39 ± 0.22 mmHg ml^{-1} min after the first and second embolization, but these differences were not significant. Average wave reflection index (R_w) was 0.66 ± 0.06 at baseline and increased significantly to 0.92 ± 0.02 and 0.92 ± 0.03 after the first and second embolizations, respectively ($P < 0.05$).

Histology

To ensure that microspheres reached both lungs in all experiments, hemotoxylin-stained sections were examined for each lung. All sections from right and left lungs showed microspheres in pulmonary vessels and not in alveolar spaces (Fig. 7), which would have been evidence of tissue damage during OCT perfusion or repositioning of spheres during sectioning and staining. Perfusion and ventilation appeared to cause minimal edema or damage to lung tissue.

DISCUSSION

Pulmonary artery and left atrial pressures in response to steady and pulsatile flows were measured before and after two infusions of $25 \mu m$ microspheres in isolated, ventilated, and perfused mouse lungs. Microsphere infusion increased P_{PA} , PVR, pulmonary vascular impedance at 0 Hz, and low frequencies, and shifted f_{\min} to higher frequencies. Our results demonstrate that steady and pulsatile pressure-flow rate relationships can be measured in isolated, ventilated, and perfused mouse lungs, and that embolic pulmonary hypertension has similar effects in mice as in larger animals.

Initial Measurements

At baseline, pulmonary artery pressure measured before pulsatile perfusion was approximately 11 mmHg at a flow rate of 1 ml/min; recent studies in isolated, ventilated, and perfused mouse lungs have shown similar baseline pressures despite differences in perfusate and mouse strain.^{1,10,27} With microsphere embolization, P_{PA} increased significantly. An increase in P_{PA} with microsphere embolism previously has been measured in larger animal models including rats, dogs, goats, and pigs.^{3,6,11,22,26,29,32} Also, on average, the initial P_{PA} was higher than that measured at the same flow rate after pulsatile perfusion. This finding suggests that preconditioning with pulsatile perfusion decreases resistance and should be performed prior to data collection in isolated lung experiments.

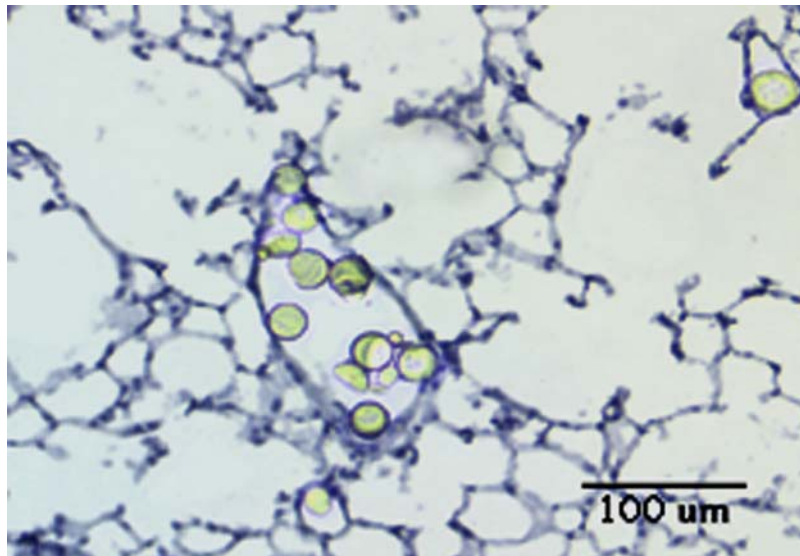


FIGURE 7. Representative histological section (hematoxylin stained) of lung parenchyma showing microspheres in large and small pulmonary arteries. Scale bar is 100 μm .

Steady Pressure-Flow Rate Relationships

At baseline conditions, the difference between P_{PA} and P_{LA} , or ΔP was nearly constant as flow rate increased from 1 to 5 ml/min. By contrast, Parker et al. found that ΔP increased slightly for increasing flow rates in isolated mouse lungs, but only investigated between 0.3 and 1.0 ml/min.²⁷ At higher flow rates, such as those used in our study, capillary recruitment, distention, and a shift in lung zones (from 1 at low flows to 3 at high flows) may account for the constancy of ΔP with increasing flow.³⁰ After embolization, ΔP increased with increasing flow rates, suggesting that the recruitment of capillaries and distension of microvessels could not compensate completely for the obstruction caused by emboli in the lungs. Hence, larger pressure drops across the pulmonary vascular network were generated, which increased with increasing flow rate.

For all conditions, PVR decreased with increasing flow rate. The PVR after both embolizations were higher than at baseline for all flow rates examined. This last finding is consistent with previous research in larger animal models in which the lungs were embolized with 15 μm microspheres,¹¹ 100 μm glass beads,^{5,6,26} 0.5 mm glass beads,³² and autologous blood clot ($<1 \text{ cm}^3$).¹³ While each infusion of 1×10^6 25 μm microspheres increased PVR, the changes from the first embolization to the second (as a function of flow rate) were not statistically significant. Glennly *et al.* found a linear relationship between the number of 15 μm -diameter microspheres infused into isolated rat lungs and the increase in pulmonary vascular resistance.¹¹ An important scaling factor is likely the ratio of infused solid volume to circulating lung blood volume. While the equivalent solid volumes infused were similar (a maximum of

8.8 mm^3 in [11] vs. 8.2 and 1.64 mm^3 , after embolism I and II, respectively), the rat circulating blood volume is clearly larger. Thus, taken together, these studies suggest that at low ratios of solid to lung blood volume, resistance increases linearly with solid volume infused but that at high ratios the relationship is sublinear.

Pulsatile Pressure-Flow Rate Relationships

At baseline, the change in impedance as a function of frequency was as follows: the highest impedance value occurred at 0 Hz (Z_0), followed by a minimum at 5 Hz, and a local maximum at 15 Hz. The existence of a maximum at 0 Hz followed by a minimum and fluctuations at higher frequencies is the classic pulmonary vascular impedance pattern, and is consistent with many other studies in animals and humans.^{8,16,18,20,26,30,32} After embolization, Z_0 increased significantly compared to baseline. This increase represents the increased opposition to mean flow through the pulmonary vascular system due to the microsphere emboli. Under pulsatile flow conditions, with a mean flow rate of 3 ml/min, Z_0 at baseline and after embolization were comparable to PVR at the same flow rate and condition. Therefore, the overall resistive response of the lungs was similar whether steady or pulsatile flow was used. An increase in Z_0 with microsphere, glass bead, and autologous blood clot embolization previously has been measured in larger animal models including dogs, goats, and pigs.^{3,18,22,26,32}

The characteristic impedance Z_C did not vary significantly after embolization, but did show a slight decreasing trend. Changes in Z_C after pulmonary embolization

have been shown to differ with species. For example, Z_C in dog lungs decreased after pulmonary embolization with 0.5 mm or 100 μm glass beads or autologous blood clots.^{8,18,22,26,32} However, in species with higher pulmonary vascular reactivity such as pigs and goats, Z_C increased.^{18,32} Others have suggested that this species-dependency of Z_C is due to passive vessel distension, the capacity for which is species dependent.^{3,18,32} Characteristic impedance is also calculated over varying frequency ranges: 2–12 Hz², above 2 Hz²³ and above the frequency of the first minimum.¹⁹ We chose to calculate Z_C by using the frequencies above the first minimum,²⁵ which was approximately 5 Hz at baseline.

More insight into the changes in the pulmonary vasculature with embolization can be gained from an in-depth analysis of the frequency-dependent changes in the pulmonary vascular impedance spectrum, such as is being pursued for clinical application.¹⁴ In particular, f_{\min} and R_w are related to the major reflecting sites in the pulmonary vascular network.²⁰ In this study, f_{\min} increased with embolization, from 5 Hz to at least 20 Hz. In the healthy lungs of dogs, minipigs, and humans, f_{\min} is in the 2–4 Hz range^{18,20} whereas after embolization in dogs and minipigs, f_{\min} shifts to 5–12 Hz.^{7,8,18,22} This increase in f_{\min} with embolization is due to a more proximal location of the major reflecting sites in the pulmonary arteries.⁷ The increase in calculated index of wave reflection with embolization, which also has been shown to occur in larger animal models,^{8,18} is consistent with a more proximal location of the major reflecting sites. In healthy animals, f_{\min} varies due to differences in the location of wave reflection sites as a function of animal size and vascular anatomy, and tends to be higher for smaller animals.²⁰

The shift in the location of major reflecting sites should be a function of the size and distribution of emboli. To further explore this issue, we investigated the distribution of emboli by quantifying the percent obstructed area of vessels in the histological sections obtained as described above. In particular, for each lung cross-section, fields of view were inspected for vessels containing microspheres. A random sample of at least 14 vessels containing microspheres was chosen for quantification. The area of the lumen was measured with quantitative image analysis tools (MetaVue), and the obstructed area was measured with color thresholding for the microspheres. The percent obstructed area was calculated as the ratio of obstructed area to total luminal area ($\times 100$). The average diameter was calculated as the average lumen height and width measured with line tools. Vessels with aspect ratios greater than 2 were excluded. The percent obstructed area decreased rapidly with increasing average vessel diameter (Fig. 8). The considerable obstruction by the microsphere emboli in vessels less than 100 μm in diameter clearly represents new reflection sites after embolization, which are more proximally located than the capillary bed. These new sites are likely responsible for increased

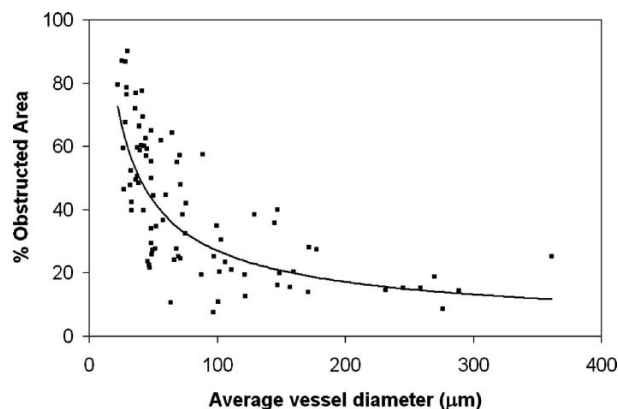


FIGURE 8. Percent obstructed area versus average vessel diameter (D) after second embolization as measured from histological sections from all six animals. Best fit power function trendline shown.

Z values at low frequencies. We might speculate that if all the microspheres had completely blocked vessels of 50 μm diameter, there would have been a sharp peak in impedance at one frequency between 2 and 15 Hz. However, since there was a continuous distribution of size of vessels that were blocked, there was also a continuous distribution of reflection sites after embolization and a gradual decrease in Z with frequency between 2 and 15 Hz.

Experimental Considerations

Vascular smooth muscle contraction as a function of pressure, flow rate, or embolization was not assessed in this study and cannot be discounted because of the availability of calcium (100 mg/L calcium nitrate tetrahydrate) in the RPMI media. Contraction of smooth muscle cells could have been eliminated by using a calcium-free solution as a perfusate or by using a vasodilator such as papaverine. Alternatively, the impact of smooth muscle cell contraction could have been assessed by adding vasoconstrictors such as norepinephrine or serotonin to the perfusate. However, our goal was to determine the effects of emboli on P_{PA} , PVR, and the impedance spectrum in the presence of normal vascular tone.

In all isolated lung systems, the measured pressures depend on the choice of perfusate, in particular its viscosity. The 3.5% Ficoll in RPMI perfusate was chosen based on previous isolated lung studies^{10,31,33} and as mentioned above, the pressures obtained here were comparable at the same flow rates. The viscosity of the Ficoll-RPMI perfusate was approximately 3-fold lower than blood: 1.1 cP compared to about 3.5 cP commonly reported for blood. Dextran was used to increase viscosity in preliminary experiments, but there was a high prevalence of edema in the lungs with this perfusate.

Subphysiological flow rates also were used to prevent edema. The isolated, perfused mouse lung system was developed for steady flow perfusion, and has most often been used at very low flow rates (≤ 1 ml/min).^{1,27,31} A recent study of hypoxic pulmonary vasoconstriction with various perfusates in an isolated lung system used both 1 ml/min and 3 ml/min steady flow rates without reported edema.³³ The flow rates used in this study (1–5 ml/min) were experimentally determined to cover as much of the physiologic range as possible without compromising lung function. In preliminary experiments, higher flow rates, especially under steady flow conditions, generally caused rapid and irreversible edema.

In this isolated lung study, measurements were taken when lungs were inflated to an end-inspiratory airway pressure $P_{\text{air}} = 10$ cmH₂O, or ~ 7.4 mmHg. We used end-inspiratory instead of end-expiratory pressure because in preliminary experiments (without Ficoll), taking measurements at lower pressures occasionally led to irreversible edema. For steady flow perfusion greater than 3 ml/min, P_{LA} was greater than P_{air} and thus the lungs were in zone 3 conditions at baseline and after each embolization. However, for steady flow perfusion at 3 ml/min or less, zone 1 conditions likely occurred. As mentioned above, the shift from zone 1 to zone 3 conditions may have affected the pulsatile pressure-flow rate relationships found here. Also, zone 1 conditions may have occurred during pulsatile perfusion especially at transiently low flow rates. Nevertheless, since the capillaries are distal to the emboli and the pressure changes caused by the emboli, the capillary perfusion pressures should be comparable at baseline and after embolization. Thus, the shifts from zone 1 to 2 to 3 conditions should occur at comparable flow rates, and the significance differences between baseline and embolization found here should hold.

CONCLUSIONS

In this study, we demonstrated that pulsatile flow can be used in an isolated, ventilated, and perfused mouse lung to characterize the pulsatile pressure-flow rate relationships in the mouse pulmonary vascular network. Our results demonstrate that pulmonary artery pressure, resistance, and impedance increased with pulmonary embolization in ways consistent with *in vivo* studies in larger animals and humans. In particular, the pressure drop across the pulmonary vascular network and PVR increased after embolization, and frequency-dependent features of the pulmonary vascular impedance spectrum were suggestive of shifts in the locations of the major pulmonary vascular reflection sites with embolization. The flow- and frequency-dependent changes we found demonstrate the usefulness of the isolated, ventilated, and perfused mouse lung for investigations into both steady and pulsatile pressure-flow rate relationships in the mouse.

ACKNOWLEDGMENTS

This research was supported by the Whitaker Foundation (Biomedical Engineering Research Grant RG-02-0618). The authors would like to thank Nidal E. Muvarak for his excellent tissue preservation and histology work and Rebecca Vanderpool for additional technical assistance.

REFERENCES

- 1 Archer, S. L., H. L. Reeve, E. Michelakis, L. Puttagunta, R. Waite, D. P. Nelson, M. C. Dinauer, and E. K. Weir. O₂ sensing is preserved in mice lacking the gp91 phox subunit of nadph oxidase. *Proc. Natl. Acad. Sci. USA* 96:7944–7949, 1999.
- 2 Bergel, D. H., and W. R. Milnor. Pulmonary vascular impedance in the dog. *Circ. Res.* 16:401–415, 1965.
- 3 Calvin, J. E. Jr., R. W. Baer, and S. A. Glantz. Pulmonary artery constriction produces a greater right ventricular dynamic afterload than lung microvascular injury in the open chest dog. *Circ. Res.* 56:40–56, 1985.
- 4 Caro, C. G., and D. A. McDonald. The relation of pulsatile pressure and flow in the pulmonary vascular bed. *J. Physiol.* 157:426–453, 1961.
- 5 Ehrhart, I. C., W. M. Granger, and W. F. Hofman. Effects of arterial pressure on lung capillary pressure and edema after microembolism. *J. Appl. Physiol.* 60:133–140, 1986.
- 6 Ehrhart, I. C., and W. F. Hofman. Segmental vascular pressures in lung embolism. *J. Appl. Physiol.* 74:2502–2508, 1993.
- 7 Elkins, R. C., M. D. Peyton, and L. J. Greenfield. Pulmonary vascular impedance in chronic pulmonary hypertension. *Surgery* 76:57–64, 1974.
- 8 Ewalenko, P., S. Brimiouille, M. Delcroix, P. Lejeune, and R. Naeije. Comparison of the effects of isoflurane with those of propofol on pulmonary vascular impedance in experimental embolic pulmonary hypertension. *Br. J. Anaesth.* 79:625–630, 1997.
- 9 Fagan, K. A., M. Oka, N. R. Bauer, S. A. Gebb, D. D. Ivy, K. G. Morris, and I. F. McMurtry. Attenuation of acute hypoxic pulmonary vasoconstriction and hypoxic pulmonary hypertension in mice by inhibition of rho-kinase. *Am. J. Physiol. Lung Cell Mol. Physiol.* 287:L656–664, 2004.
- 10 Fagan, K. A., R. C. Tyler, K. Sato, B. W. Fouty, K. G. Morris Jr., P. L. Huang, I. F. McMurtry, and D. M. Rodman. Relative contributions of endothelial, inducible, and neuronal nos to tone in the murine pulmonary circulation. *Am. J. Physiol.* 277:L472–478, 1999.
- 11 Glenny, R. W., S. L. Bernard, and W. J. Lamm. Hemodynamic effects of 15-microm-diameter microspheres on the rat pulmonary circulation. *J. Appl. Physiol.* 89:499–504, 2000.
- 12 Hasegawa, J., K. F. Wagner, D. Karp, D. Li, J. Shibata, M. Heringlake, L. Bahlmann, R. Depping, J. Fandrey, P. Schmucker, and S. Uhlig. Altered pulmonary vascular reactivity in mice with excessive erythrocytosis. *Am. J. Respir. Crit. Care Med.* 169:829–835, 2004.
- 13 Hasinoff, I., J. Ducas, U. Schick, and R. M. Prewitt. Pulmonary vascular pressure-flow characteristics in canine pulmonary embolism. *J. Appl. Physiol.* 68:462–467, 1990.
- 14 Huez, S., S. Brimiouille, R. Naeije, and J. L. Vachiery. Feasibility of routine pulmonary arterial impedance measurements in pulmonary hypertension. *Chest* 125:2121–2128, 2004.
- 15 Kafi, S. A., C. Melot, J. L. Vachiery, S. Brimiouille, and R. Naeije. Partitioning of pulmonary vascular resistance in primary

- pulmonary hypertension. *J. Am. Coll. Cardiol.* 31:1372–1376, 1998.
- ¹⁶Kussmaul, W. G., A. Noordergraaf, and W. K. Laskey. Right ventricular-pulmonary arterial interactions. *Ann. Biomed. Eng.* 20:63–80, 1992.
- ¹⁷Littler, C. M., K. G. Morris Jr., K. A. Fagan, I. F. McMurtry, R. O. Messing, and E. C. Dempsey. Protein kinase c-epsilon-null mice have decreased hypoxic pulmonary vasoconstriction. *Am. J. Physiol. Heart Circ. Physiol.* 284:H1321–1331, 2003.
- ¹⁸Maggiorini, M., S. Brimiouille, D. De Canniere, M. Delcroix, and R. Naeije. Effects of pulmonary embolism on pulmonary vascular impedance in dogs and minipigs. *J. Appl. Physiol.* 84:815–821, 1998.
- ¹⁹McDonald, D. A. *Blood Flow in Arteries*. London: Edward Arnold, 1974.
- ²⁰Milnor, W. R., *Hemodynamics*. Baltimore, MD: Williams & Wilkins, 1989.
- ²¹Naeije, R. Pulmonary vascular resistance. A meaningless variable. *Intensive Care Med.* 29:526–529, 2003.
- ²²Naeije, R., J. M. Maarek, and H. K. Chang. Pulmonary vascular impedance in microembolic pulmonary hypertension: Effects of synchronous high-frequency jet ventilation. *Respir. Physiol.* 79:205–217, 1990.
- ²³Nichols, W. W., C. R. Conti, W. E. Walker, and W. R. Milnor. Input impedance of the systemic circulation in man. *Circ. Res.* 40:451–458, 1977.
- ²⁴Nichols, W. W., and M. F. O'Rourke. *McDonald's Blood Flow in Arteries: Theoretical, Experimental, and Clinical Principles*. New York: Oxford University Press, 2005.
- ²⁵Nichols, W. W., M. F. O'Rourke, C. Hartley, and D. A. McDonald. *McDonald's blood flow in arteries: Theoretical, experimental, and clinical principles*. New York: Oxford University Press, 1998.
- ²⁶Pagnamenta, A., P. Fesler, A. Vandinivit, S. Brimiouille, and R. Naeije. Pulmonary vascular effects of dobutamine in experimental pulmonary hypertension. *Crit. Care Med.* 31:1140–1146, 2003.
- ²⁷Parker, J. C., M. N. Gillespie, A. E. Taylor, and S. L. Martin. Capillary filtration coefficient, vascular resistance, and compliance in isolated mouse lungs. *J. Appl. Physiol.* 87:1421–1427, 1999.
- ²⁸Reeves, J. T., J. H. Linehan, and K. R. Stenmark. Distensibility of the normal human lung circulation during exercise. *Am. J. Physiol. Lung Cell Mol. Physiol.* 288:L419–425, 2005.
- ²⁹Riegger, G. A., and P. Hoferer. A new experimental model for measurement of pulmonary arterial haemodynamic variables in conscious rats before and after pulmonary embolism and during general anaesthesia. *Cardiovasc. Res.* 24:340–344, 1990.
- ³⁰Taylor, A. E. *Clinical Respiratory Physiology*. Philadelphia, PA: Saunders, 1989.
- ³¹von Bethmann, A. N., F. Brasch, R. Nusing, K. Vogt, H. D. Volk, K. M. Muller, A. Wendel, and S. Uhlig. Hyperventilation induces release of cytokines from perfused mouse lung. *Am. J. Respir. Crit. Care Med.* 157:263–272, 1998.
- ³²Wauthy, P., A. Pagnamenta, F. Vassalli, R. Naeije, and S. Brimiouille. Right ventricular adaptation to pulmonary hypertension: An interspecies comparison. *Am. J. Physiol. Heart Circ. Physiol.* 286:H1441–1447, 2004.
- ³³Weissmann, N., E. Akkayagil, K. Quanz, R. T. Schermuly, H. A. Ghofrani, L. Fink, J. Hanze, F. Rose, W. Seeger, and F. Grimminger. Basic features of hypoxic pulmonary vasoconstriction in mice. *Respir. Physiol. Neurobiol.* 139:191–202, 2004.
- ³⁴Zhao, L., N. A. Mason, N. W. Morrell, B. Kojonazarov, A. Sadykov, A. Maripov, M. M. Mirrakhimov, A. Aldashev, and M. R. Wilkins. Sildenafil inhibits hypoxia-induced pulmonary hypertension. *Circulation* 104:424–428, 2001.